Molecular Ecology (2001) **10**, 1563–1576

Spatial analysis of allozyme and microsatellite DNA polymorphisms in the land snail *Helix aspersa* (Gastropoda: Helicidae)

J.-F. ARNAUD,*† L. MADEC,* A. GUILLER† and A. BELLIDO‡
UMR CNRS 6553, Service de Zoologie et Ecophysiologie, Université de Rennes 1, Campus de Beaulieu, Avenue du Gal Leclerc, 35042 Rennes cedex, †UMR CNRS 6553, Service de Parasitologie Pharmaceutique, Université de Rennes 1, Avenue du Pr. Léon Bernard, 35043 Rennes cedex, ‡UMR CNRS 6553, Service d'Ecologie du sol et de Biologie des Populations, Station Biologique de Paimpont, 35380 Plélan-le-Grand, France

Abstract

The genetic structure of the land snail *Helix aspersa* was investigated for 21 populations collected along a road located in the polders of the Bay of Mont-Saint-Michel (Brittany, France), following a sampling scheme the area of which did not exceed 900 m in length. A total of 369 individuals were genotyped for five enzymatic markers and seven microsatellite loci. We used sequential hierarchical *F*-statistics at different spatial scales and spatial autocorrelation statistics to explore recent historical patterns involved in the observed genetic distribution. Whatever the statistics used, congruent levels of spatial genetic substructuring across loci were demonstrated, excepted for one allozyme locus. Overall spatial genetic arrangement matched in a substantial fashion theoretical predictions based on the limited dispersal power of land snails. Positive autocorrelation over short-distance classes may result from the development of genetically distinct patches of individuals organized in family-structured colonies. Therefore, spatial signatures of average *I* correlograms can be viewed as the expression of a stepping-stone model of population structure, sometimes involving external migrational events. Overall, the revealed pattern of population subdivision on a microgeographical scale was suggestive of a neighbourhood structure. Finally, microsatellite loci are especially suitable for the detection of small genetic clustering, and combining different classes of markers offers the potential to gain further insight into the description of spatial genetic variability over short temporal and geographical scales.

Keywords: allozymes, *F*-statistics, genetic structure, land snail, microsatellites, spatial autocorrelation

Received 7 October 2000; revision received 11 January 2001; accepted 17 January 2001

Introduction

The description of patterns of genetic variation provides key features from the evolutionary forces that shape the structure of natural populations. Species rarely consist of a single large population, but rather are subdivided into numerous local subpopulations (or demes) mainly because of landscape fragmentation (McCauley 1995). Within this context, spatial distribution of genetic diversity within and among populations is intrinsic to population genetic processes. Thus, patterns of genetic structure can be attributed to the effects of natural selection, mutation, genetic drift and gene flow (Slatkin 1994; Hamrick & Nason 1996; Allendorf & Seeb 2000; Hedrick 2000). In turn, these evolutionary components are influenced by life history features such as breeding systems and behavioural traits as well as by dispersal abilities. With respect to the latter point, limited dispersal ability can result in matings among related individuals. When such consanguineous matings by proximity are repeated over generations, theoretical and empirical studies predict the build-up of marked genetic isolation by distance and striking spatial patterns of genetic variation (Sokal & Wartenberg 1983; Epperson 1995; Streiff *et al*. 1998; Epperson *et al*. 1999; Hardy & Vekemans 1999; Williams & Waser 1999; Takahashi *et al*. 2000; Ueno *et al*. 2000).

Because of their well-known low ability for dispersal, land snails are especially appropriate to study a neighbourhood

Correspondence: Jean-François Arnaud. Fax.: + 33 (0)2–99–28–16–12; E-mail: jarnaud@univ-rennes1.fr

population structure and the effects of strong population subdivision (Selander & Ochman 1983; Schilthuizen & Lombaerts 1994; Pfenninger *et al*. 1996). Indeed, most land snail species live in discrete aggregated populations, have a sedentary nature related to a marked homing behaviour and their dispersal capabilities are set against the cost of locomotion which is excessively high in terrestrial pulmonates (Denny 1980; see also Madec *et al*. 2000). Such biological traits, in relation to a low amplitude for trivial movements, may lead to substantial genetic differentiation and population substructuring, even over a very short spatial scale of investigation (Selander & Kaufman 1975; Selander & Ochman 1983; Pfenninger *et al*. 1996; Arnaud *et al*. 1999a,b).

The present study focuses on population genetics, at a microgeographical scale, in the garden snail *Helix aspersa* (Müller). This snail has successfully colonized a large range of man-disturbed habitats in Western Europe and is considered an important pest in countries where it is a recent introduction, especially in Australia and New Zealand (Rudman 1999; Madec *et al*. 2000; Winston Ponder, personal communication). This paper aims to characterize the spatial distribution of allelic frequencies in colonies of *H. aspersa* sampled in a small area of the polders of the Bay of Mont-Saint-Michel (France). This site has been recently colonized by this snail and constitutes a complex mosaic of agricultural human-modified environments. At the scale of the whole polders area, *H. aspersa* occurs in patchily distributed populations and this situation seems representative for a metapopulation structure in a heterogeneous landscape (Arnaud 2000). However, the colonies sampled for the present study are localized within a strongly restricted area that constitutes a continuous environment, i.e. along a road's edge within a ditch. The choice of this microgeographical sampling strategy allows us to eliminate problems associated with highly fragmented habitats which are likely to blur fine-scale patterns of genetic arrangement among nearby populations (e.g. Arnaud *et al*. 1999b). Hence, it allows the study of microcontinuously distributed populations with a sampling scheme appropriate to test for an isolation by distance model of population genetic structure.

As few allozyme loci remain polymorphic at such a fine-scale of investigation, we also used microsatellite markers recently developed by Guiller *et al*. (2000). Such short stretches of repeated DNA generally display an exceptional polymorphism, so that microsatellites have become, in recent years, the markers of choice for population genetic studies (Estoup & Cornuet 1999) or phylogenetic inferences (Kirchman *et al*. 2000; Zhu *et al*. 2000). Our main purpose is to describe the spatial structure of allozyme and microsatellite loci in *H. aspersa* and to test if discordances in patterns of genetic structure are revealed using both types of markers. We used sequential hierarchical *F*-statistics to depict patterns of differentiation at different spatial scales. Indirect estimates of gene flow using the statistics of population differentiation (i.e. *Nm*) were not calculated, because the assumptions underlying such estimates are generally violated in natural populations (McCauley 1995; Whitlock & McCauley 1999). Instead, spatial genetic distribution was analysed using spatial autocorrelation statistics that have become widely used to characterize the population genetic structure of various animal and plant species (Bacilieri *et al*. 1994; Streiff *et al*. 1998; Arnaud *et al*. 1999a,b; Reusch *et al*. 1999; Williams & Waser 1999; Takahashi *et al*. 2000; Ueno *et al*. 2000) and are still subject to theoretical developments (e.g. Sokal *et al*. 1997; Epperson *et al*. 1999; Hardy & Vekemans 1999; Smouse & Peakall 1999).

Materials and methods

Study site and sampling design

Twenty-one colonies were sampled within a ditch, along a road located in the polders of the Bay of Mont-Saint-Michel (Brittany, northwestern France), following a sampling scheme the area of which did not exceed 900 m in length (Fig. 1). Sample colonies were obtained from a very restricted area to ensure that individuals belonged to the same breeding group: each colony was composed of snails collected in regularly spaced pipes that form hospitable resting sites as well as aestivating or hibernating refuges (see Fig. 1). Hence, as the ditch is a continuous environment, the only heterogeneity consists of the regular occurrence of pipes that mimics a stepping-stone arrangement of hospitable sites. Throughout this study, a colony will be defined as a set of individuals that live in the same pipe, i.e. a population spatially well circumscribed and of limited size according to Lamotte (1951). Samples were collected on the same day (June 1998) under dry conditions, when the snails were inactive. The effectiveness of the sampling procedure was verified by a second census that yielded only some new born snails. Genotypes were obtained from a total of 369 snails and sample sizes ranged from 10 to 25 individuals per population (see Arnaud 2000).

Allozyme and microsatellite analysis

Allozyme genotypes at five polymorphic enzyme loci (*Lap-2*, *Est-3*, *Aat-1*, *Mdh-1* and *Pgm-2*) were determined by means of starch and polyacrylamide gel electrophoresis. Detailed procedures and genetic interpretations of zymograms are given in Madec (1991) and Guiller *et al*. (1994).

To examine microsatellite variability, DNA for genotyping was extracted using a 10% Chelex-100 suspension as described by Estoup *et al*. (1996). Seven microsatellite loci (*Ha2*, *Ha5*, *Ha6*, *Ha8*, *Ha10*, *Ha11* and *Ha13*) were selected for their high polymorphism. Details of protocols for primers development and methods of amplification of DNA samples are reported in Arnaud (2000) and Guiller *et al*. (2000).

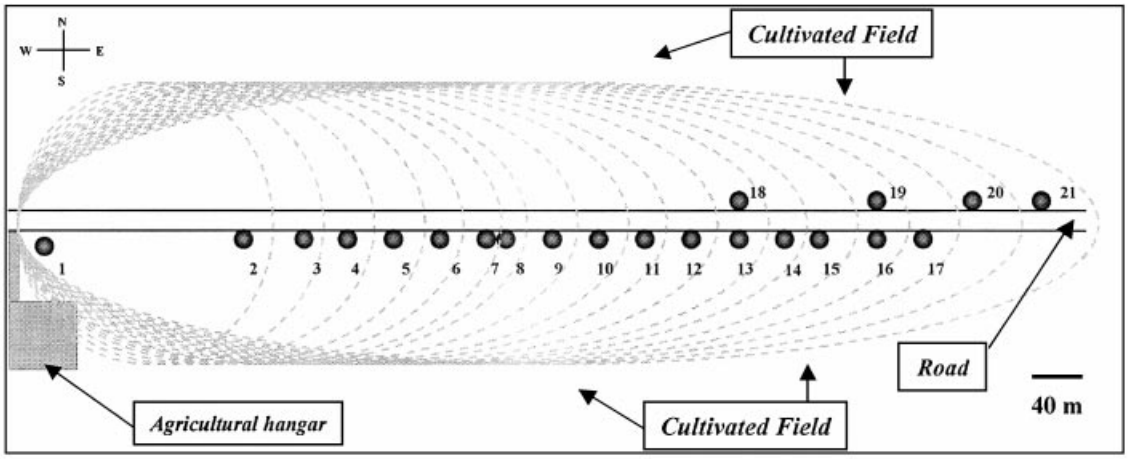

Fig. 1 Map of sample locations numbered from 1 to 21. The distribution of snails is strictly restricted to the boundary of the ditch because the area surrounding the road is inhospitable. Thin lines show the successive sequential groupings of the 21 samples used for spatial differentiation statistics. Such subdivisions allow the calculation of *F*-statistics for 18 distance classes corresponding to the geographical co-ordinates of each colony.

Statistical methods

Genetic diversity, genotypic phase disequilibrium, within-sample deviation from Hardy–Weinberg equilibrium and global differentiation among colonies have been previously investigated (Arnaud 2000; Arnaud, unpublished results). There was no evidence for linkage between any of the pairs of loci. Allozyme and microsatellite genotype proportions were largely concordant with those expected under the Hardy–Weinberg equilibrium within almost all colonies, and strong concordance was found across the two categories of markers in the amount and pattern of overall genetic variation.

Spatial statistics. Spatial autocorrelation methods were used to investigate the spatial distribution of allelic frequencies among colonies. Spatial autocorrelation is defined as the association of the values of one geographically distributed variable with the values of the same variable at other localities (Sokal & Oden 1978). Thus, spatial autocorrelation coefficients efficiently summarize the strength of allele frequency association between pairs of sample populations as a function of their geographical distance or, in other words, are the expression of similarities between neighbouring locations (Sokal & Oden 1978; Sokal *et al*. 1997). In this way, spatial patterns produced by distinct classes of evolutionary processes can be described and recognized (Sokal & Wartenberg 1983; Sokal *et al*. 1989, 1997). Here, we used the Moran's *I* coefficient:

$$I_k = [n\sum_{i\neq j} w_{ij}^{(k)}(x_i-\bar{x})(x_j-\bar{x})]/[\sum_{i\neq j} w_{ij}^{(k)}\sum_i (x_i-\bar{x})^2]$$

where n is the number of sampled localities, $\bar{x}$ is the mean value of x_i, k is the distance class, and $w_{ij}^{(k)}$ is the join matrix, being set to unity if i and j are both in class k, and 0 otherwise. Rare alleles are not very informative on spatial processes, since their patterns are greatly affected by the random effects of sampling (Sokal & Oden 1978; Sokal *et al*. 1989). Thus, Moran's *I* values were calculated only for the most frequent alleles at each locus in order to maintain the statistical independence of our tests. For diallelic loci (i.e. *Aat-1* and *Pgm-2*), the autocorrelation coefficients for each allele are identical, so that only Moran's *I* value of the most common allele is presented. Significance levels of individual autocorrelation coefficients were tested against the null hypothesis of no spatial arrangement by resampling procedure (1000 permutations). Each permutation consisted of a random redistribution of sample colonies over spatial co-ordinates and the observed *I* was then compared with the empirical distribution after randomization.

Autocorrelation statistics were estimated using the between-population linear distance criterion and 14 continuous distance classes of 50 m were considered, from 0–50 m to 650–700 m. The last distance classes were not taken into account in analyses because too few pairs of localities were involved in the calculations. The set of autocorrelation coefficients at various distance classes, or correlogram, objectively describes the geographical pattern of an allele frequency which, in turn, can often be associated with a generating process. Overall significance of the entire correlograms was evaluated using the Bonferroni technique (Oden 1984). To summarize information provided by alleles, mean values of individual Moran's *I* were calculated for each locus as the arithmetic average over alleles to produce consensus correlograms (Reusch *et al*. 1999; Williams & Waser 1999; Takahashi *et al*. 2000; Ueno *et al*. 2000). Moran's *I* were also calculated for strict nearest-neighbour pairs of colonies according to the Gabriel network which postulates that any two localities A and B are considered as connected if no other locality lies on or within the circle whose diameter

is the line AB ($d^2_{AB} < d^2_{AC} + d^2_{BC}$) (Gabriel & Sokal 1969). All Moran statistics and their statistical significances were calculated using AUTOCOR, a program written by A. B.

Hierarchical F-*statistics*. Goudet *et al*. (1994) proposed a graphical method to assess the levels at which a population is structured. The principle consists in sequentially pooling sample populations by increasing the size of subdivision so that one (or more) new populations is included in the precedent pooling and new fixation indices are then calculated. The procedure is repeated until all samples are pooled together, leading to the last estimate, F_{IT}. The different estimates are plotted on a graph, the *x*-axis representing the different levels of pooling and the *y*-axis the equivalent *F*-values. Such a pooling scheme is often subjective but usually, as noted by Goudet *et al*. (1994), grouping based on geographical distances between subpopulations is generally a good strategy (see also Bacilieri *et al*. 1994; Chapuisat *et al*. 1997; and Streiff *et al*. 1998). Our sample collection is particularly well suited to this type of analysis because we restricted the size of sample sites and we had a precise record of the geographical co-ordinates of colonies.

F-statistics were computed according to the ANOVA procedure of Weir & Cockerham (1984) using the software FSTAT, version 1.2 (Goudet 1995). Permutation testing was used to determine whether observed values of F_{IS} and F_{ST} were significantly different from 0 by resampling 3000 times the alleles within samples (F_{IS}) or among samples (F_{ST}). For each sequential grouping, confidence intervals for the means of F_{IS} and F_{ST} values were obtained by bootstrapping over loci.

To estimate genetic differentiation over different spatial scales, fixation indices were calculated for two distinct subdivisions of the prospected area. The first one consisted of considering all the sampled colonies separately (distance class = 0), then pooling sample colonies 1 and 2 for the following distance class (that corresponds to the physical distance between these two colonies, i.e. 174 m), colonies 1, 2 and 3 for the next one, and so on until only two groups remain (that is, all colonies pooled excepted colony 21, see Fig. 1). At each pooling stage, the to-be-pooled sample colonies are still considered as all distinct. Such a sequential grouping scheme allowed us to calculate *F*-statistics for 18 precise distance classes that correspond to the geographical coordinates of each colony added during the pooling stage. Note that colonies 13 and 18 are pooled together for their corresponding distance class, as well as colonies 16 and 19 also added as one (see Fig. 1).

The second pooling strategy was based on the genetic relationships previously depicted among the 21 colonies (Arnaud 2000). Grouping of colonies was:

0 All sample colonies independently;
1 Group A (19, 20, 21), group B (15, 16, 17), group C (13, 14, 18), group D (11, 12), group E (1, 2, 3, 4, 5) and group F (6, 7, 8, 9, 10);
2 Groups (A, B) (C, D) and (E, F);
3 Groups (A, B, C, D) and (E, F).

Results

Genetic diversity

Allozyme markers displayed moderate levels of polymorphism with two or three alleles per locus for a total of 13 alleles. By contrast, microsatellite loci were highly polymorphic with an overall total of 114 alleles, number of alleles per locus ranging from five (*Ha2*) to 32 (*Ha13*). A visual example of this high allelic diversity is shown in Fig. 2.

Spatial genetic arrangement

Spatial autocorrelation analysis yielded 700 individual *I* values (Tables 1 and 2). The overall departure from the null

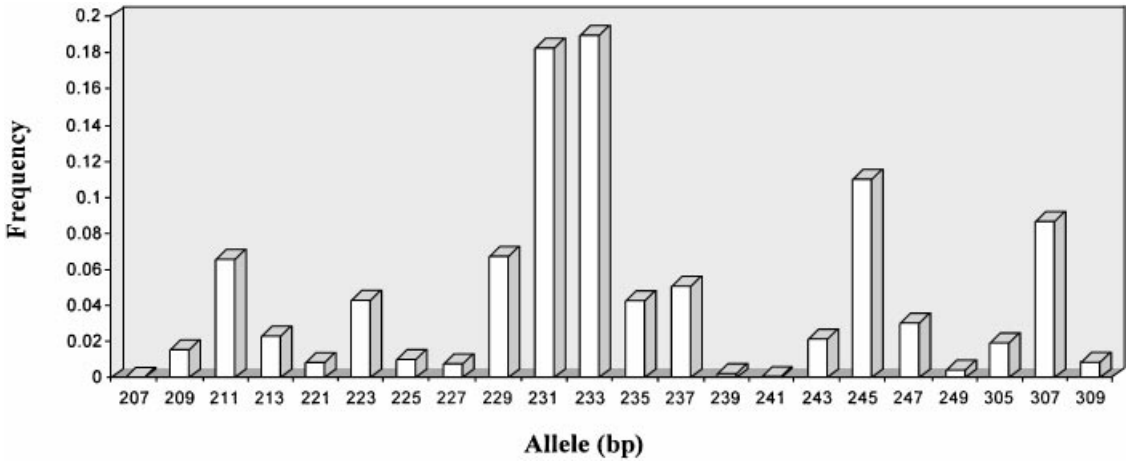

Fig. 2 Allele frequency distribution for the microsatellite locus *Ha11* in *Helix aspersa*. The name of each allele corresponds to its size in bp.

Table 1 Spatial autocorrelation analysis of frequencies of the most common alleles for seven microsatellite loci in *Helix aspersa*

Locus	Allele (bp)	Distance class limits (m)														Overall correlogram probability	Gabriel network	Pattern
		50	100	150	200	250	300	350	400	450	500	550	600	650	700			
Ha2																		
	304 *(0.10)*	0.02	0.44 **	0.20	0.04	−0.08	−0.11	−0.23	−0.15	−0.37	−0.38	−0.50	−0.79 *	−0.41	−0.53	*	0.33 *	IBD
	306 *(0.47)*	0.95 ***	0.86 ***	0.62 **	0.36 *	−0.03	−0.38	−0.79 **	−0.81 ***	−1.06 ***	−0.97 **	−0.98 **	−0.71	−0.60	−0.42	***	0.92 ***	IBD
	308 *(0.27)*	0.40 *	0.46 **	0.15	−0.12	−0.04	−0.32	−0.42	−0.34	−0.56 *	0.01	−0.14	0.28	−0.44	−1.35 *	*	0.57 ***	IBD
Ha5																		
	187 *(0.39)*	0.30	0.48 **	0.29	0.09	−0.30	−0.34	−0.58 **	−0.07	−0.41	−0.27	0.03	0.02	−0.46	−0.23	*	0.26	AIBD
	189 *(0.14)*	0.33	0.13	0.07	−0.14	−0.03	−0.35	−0.30	−0.29	−0.02	0.06	−0.11	−0.31	−0.36	1.08	NS	0.42 *	AIBD
	191 *(0.08)*	0.57 **	0.51 **	0.44 *	0.29	−0.06	−0.03	−0.44	−0.35	−0.41	−0.56 *	−0.48	−0.81 *	−1.19 **	−1.16	*	0.58 **	IBD
	195 *(0.35)*	0.68 ***	0.23	−0.08	−0.05	−0.16	−0.58 **	−0.38	−0.29	−0.19	0.14	0.48	−0.35	−0.62	1.13	***	0.43 *	AIBD
Ha6																		
	164 *(0.07)*	0.12	0.06	−0.04	−0.05	−0.07	−0.08	0.04	−0.25	−0.51 *	−0.17	−0.26	−0.19	−0.15	2.93 **	NS	0.11	AIBD
	170 *(0.50)*	0.16	0.04	−0.11	0.06	−0.12	0.04	−0.19	−0.15	0.22	0.19	0.08	−0.07	−1.33 **	−0.72	*	0.15	AIBD
	192 *(0.05)*	0.05	0.12	−0.12	−0.22	−0.31	−0.33	0.33	0.11	0.06	0.07	−0.25	0.05	0.26	0.45	NS	−0.26	S
	196 *(0.13)*	0.29	0.08	−0.03	−0.15	−0.38	−0.16	−0.51 *	−0.23	0.31	0.17	0.62 *	0.23	−0.17	0.32	NS	0.26	AIBD
	198 *(0.04)*	0.34	−0.24	−0.44 *	−0.18	0.45 *	0.03	−0.09	−0.34	−0.17	−0.03	0.26	0.12	−0.44	0.42	NS	0.10	AIBD
	200 *(0.04)*	0.13	0.33 *	−0.21	−0.08	−0.09	−0.08	−0.11	−0.12	−0.22	−0.08	−0.31	−0.06	0.04	−0.49	NS	0.58 **	AIBD
	226 (*0.07*)	0.11	−0.22	0.22	0.26	−0.37	−0.17	0.09	−0.28	0.02	−0.09	−0.03	−0.22	−0.44	0.59	NS	−0.11	S

Table 1 *Continued*

Locus	Allele (bp)	Distance class limits (m)														Overall correlogram probability	Gabriel network	Pattern
		50	100	150	200	250	300	350	400	450	500	550	600	650	700			
Ha8																		
	156 (*0.07*)	0.33	0.24	−0.01	0.04	−0.23	−0.51 *	−0.50 *	−0.16	−0.38	0.06	0.21	0.44	0.07	0.46	NS	0.33	AIBD
	158 (*0.08*)	0.18	−0.19	0.22	0.25	0.15	−0.14	0.08	−0.08	−0.26	−0.17	−0.56	−0.59	−0.55	−0.19	NS	0.21	AIBD
	162 (*0.06*)	0.30	0.35 *	0.33 *	0.46 *	0.17	−0.07	−0.17	−0.35	−0.59 *	−0.45	−1.00 *	−1.02 *	−1.01 *	−0.77	*	0.68 ***	IBD
	170 (*0.17*)	−0.43 *	0.16	−0.22	0.08	−0.07	0.28	−0.52 *	0.18	−0.09	0.02	−0.20	0.28	−0.02	−0.62	NS	−0.36	S
	172 (*0.22*)	0.41 *	0.28	0.02	0.04	−0.16	−0.18	−0.52 *	−0.32	−0.09	−0.01	−0.26	−0.26	−0.33	0.01	NS	0.29	IBD
	180 (*0.17*)	−0.44 *	−0.04	−0.04	0.06	−0.02	−0.18	0.15	0.14	0.16	−0.22	−0.20	0.10	−0.18	0.25	NS	−0.17	S
Ha10																		
	225 (*0.23*)	0.22	0.29 *	0.07	−0.25	−0.01	0.03	−0.27	−0.27	−0.60 *	−0.35	−0.08	0.00	−0.01	−0.12	NS	0.17	AIBD
	231 (*0.06*)	0.48 *	0.47 **	0.51 ***	0.13	−0.11	−0.07	−0.68 ***	−0.44	−0.73 **	−0.58 *	−0.44	−0.26	−0.54	0.01	***	0.43 *	IBD
	233 (*0.05*)	0.80 ***	0.14	−0.21	−0.31	−0.22	−0.47 *	−0.54 *	−0.48	−0.02	0.03	0.51	0.66	1.36 ***	−0.14	***	0.48 **	AIBD
	237 (*0.05*)	0.59 **	0.28	−0.11	−0.37 *	−0.34	−0.34	−0.24	−0.20	−0.08	0.09	0.11	0.22	0.09	0.07	NS	0.56 **	AIBD
	239 (*0.22*)	0.01	0.21	0.24	0.03	0.01	−0.05	−0.20	0.28	−0.24	−0.39	−0.66	−0.55	−0.02	−0.42	NS	0.25	AIBD
	241 (*0.11*)	0.70 ***	0.39 **	0.37 *	0.28	−0.18	−0.34	−0.53 **	−0.48 *	−0.57 *	−0.53	−0.77 *	−0.29	−0.26	−0.04	***	0.64 ***	IBD

Table 1 *Continued*

Locus	Allele (bp)	Distance class limits (m) 50	100	150	200	250	300	350	400	450	500	550	600	650	700	Overall correlogram probability	Gabriel network	Pattern
Ha11																		
	211 *(0.07)*	0.37	0.11	0.06	−0.12	−0.51 *	−0.44	0.02	−0.18	−0.01	0.13	−0.12	−0.19	0.40	−0.07	NS	0.45 *	AIBD
	223 *(0.04)*	0.30 *	0.06	−0.38 *	−0.18	−0.19	−0.32	−0.36	0.28	0.76 **	0.25	0.31	−0.90 **	−0.28	0.04	*	0.40 *	AIBD
	229 *(0.07)*	0.38	0.39 *	0.31	−0.13	−0.16	−0.34	−0.41	−0.54 *	−0.62 *	−0.53	−0.32	−0.23	0.86 *	0.62	NS	0.16	AIBD
	231 *(0.18)*	0.50 *	0.37 *	−0.25	−0.48 *	−0.51 *	−0.33	−0.07	0.44	0.25	−0.09	0.02	−0.70	0.12	0.36	NS	0.43 *	AIBD/S
	233 *(0.19)*	0.21	0.22	−0.18	−0.30	−0.26	−0.31	−0.06	0.04	0.29	0.23	−0.06	−0.14	−0.34	−0.04	NS	0.36 *	AIBD/S
	235 *(0.04)*	0.69 ***	0.22	−0.03	−0.19	−0.23	−0.57 ***	−0.34	−0.43 *	−0.18	−0.21	0.47	0.28	0.20	0.14	***	0.58 ***	AIBD/S
	237 *(0.05)*	0.26	−0.05	−0.11	0.32	−0.53 **	0.02	−0.34	−0.42	0.51 *	0.11	−0.18	0.20	−0.42	−0.08	*	0.14	AIBD/S
	245 *(0.11)*	0.04	−0.11	−0.04	−0.24	−0.17	0.16	0.08	0.34	−0.16	−0.51 *	−0.36	−0.19	0.26	0.78	NS	0.15	AIBD/S
	307 *(0.09)*	0.19	−0.13	−0.02	−0.13	0.01	−0.45	−0.33	0.00	0.34	0.03	0.32	0.06	0.29	−0.68	NS	0.27	AIBD/S
Ha13																		
	170 *(0.09)*	−0.14	0.38 *	0.01	−0.07	0.15	−0.22	−0.07	−0.03	−0.34	−0.47	−0.52	−0.36	−0.37	0.12	NS	0.01	S
	178 *(0.07)*	0.49 *	0.09	−0.12	−0.21	−0.05	−0.01	−0.09	−0.09	−0.14	0.19	−0.17	−0.35	−0.78 *	0.19	NS	0.43 *	AIBD
	188 *(0.31)*	0.16	0.34 *	−0.19	−0.39	−0.40	−0.25	−0.14	0.47 *	0.12	−0.05	0.24	0.29	−0.34	−0.85	NS	0.34	AIBD/S
	192 *(0.07)*	0.40 *	−0.04	−0.39	−0.24	0.01	0.42 *	0.12	0.01	−0.12	−0.09	−0.35	0.04	−0.39	−0.72	NS	0.41 *	AIBD/S
	196 *(0.11)*	0.42 *	0.57 ***	0.35 *	0.06	0.19	−0.32	−0.22	−0.49 *	−0.83 ***	−0.86 ***	−0.68 *	−0.80 *	−0.06	0.08	***	0.56 ***	IBD
	202 *(0.07)*	0.46 *	0.46 **	0.15	0.10	−0.33	−0.32	−0.65 *	−0.54 *	−0.63 *	−0.21	0.18	−0.05	0.35	0.66	NS	0.26	AIBD
	344 *(0.05)*	−0.10	0.07	−0.09	−0.05	0.06	−0.06	0.12	−0.05	0.14	−0.12	−0.61	−0.31	0.10	−0.48	NS	0.21	S

Moran's *I* are computed for 14 distance classes (linear distance criterion) and for nearest-neighbour pairs of colonies (Gabriel network). Significance of autocorrelation statistics was assessed by randomization procedures (1000 permutations). The name (in bold) of microsatellite alleles corresponds to their size in bp. Mean frequency of each allele is indicated (in italics) under their names. IBD: isolation by distance pattern; AIBD: altered isolation by distance pattern; S: stochastic variation. *$P < 0.05$; **$P < 0.01$; ***$P < 0.001$; NS: not significant.

Table 2 Spatial autocorrelation analysis of frequencies of the most common alleles for five allozymic loci in *Helix aspersa*

Locus	Allele	Distance class limits (m) 50	100	150	200	250	300	350	400	450	500	550	600	650	700	Overall correlogram probability	Gabriel network	Pattern
Lap-2																		
	100 *(0.77)*	0.31	0.09	0.22	0.05	0.03	0.14	0.39	−0.50	−0.37	−0.41	−0.55	−1.03 **	−0.31	−1.54 **	NS	0.46 *	IBD
	94 *(0.14)*	0.34	0.25	0.21	0.05	0.08	0.14	0.43 *	−0.23	−0.35	−0.80 **	−0.38	−1.00 **	−0.31	−1.52	*	0.41 *	IBD
Est-3																		
	100 *(0.69)*	−0.04	0.20	0.01	−0.09	0.12	−0.06	−0.41	0.04	−0.18	−0.27	−0.46	−0.48	0.17	−0.13	NS	0.05	AIBD/S
	95 *(0.19)*	0.59 **	0.58 **	0.47 **	0.02	−0.03	−0.29	−0.66 **	−0.73 **	−0.81 ***	−0.60	−0.84 *	−0.49	0.16	−0.41	***	0.51 *	IBD
Aat-1																		
	100 *(0.86)*	0.32 *	0.20	−0.01	0.18	0.27	−0.21	−0.42	−0.15	−0.17	−0.03	−1.34 ***	0.07	0.28	−1.10	***	0.05	AIBD
Mdh-1																		
	100 *(0.69)*	−0.16	−0.03	−0.06	−0.18	−0.19	0.29	−0.14	−0.31	0.15	−0.25	0.58	0.54	−0.28	0.19	NS	−0.07	S
	90 *(0.25)*	−0.12	0.06	−0.23	−0.26	−0.12	0.18	0.03	−0.09	−0.08	−0.17	0.64 *	0.57	−0.40	−0.21	NS	−0.05	S
Pgm-2																		
	100 *(0.64)*	0.12	0.32 *	0.16	0.39 *	−0.21	−0.02	−0.29	−0.19	−0.69 *	−0.18	−0.47	−0.19	−0.50	−0.81	NS	0.28	AIBD

Moran's *I* are computed following the linear distance criterion (14 distance classes) and according to the Gabriel network. Significance of autocorrelation statistics was assessed by randomization procedures (1000 permutations). The name (in bold) of alleles corresponds to their relative mobility. Mean frequency of each allele is indicated (in italics) under their names. IBD: isolation by distance pattern; AIBD: altered isolation by distance pattern; S: stochastic variation. *$P < 0.05$; **$P < 0.01$; ***$P < 0.001$; NS: not significant.

hypothesis of no spatial structure was significant for 18 (36%) of the individual correlograms (Bonferroni procedure). In most cases, autocorrelation tended to be significant and positive at short distances with 20 (40%) significant *I* values for the first distance class and 18 (36%) for the second. Whereas some alleles reflected a statistically significant monotonic decrease in Moran's *I* values (e.g. alleles *Ha2*^{306}, *Ha5*^{191}, *Ha8*^{162}, *Ha10*^{241}, *Ha13*^{196}, *Lap-2*^{100}, or *Est-3*^{95}), it was evident that such a pattern was blurred by stochastic variations for the other alleles, especially at longer distance classes. Therefore, the less frequent microsatellite alleles tended to be clumped for shortest scales, as shown by positive *I* values occurring at the first distance class, tapering off to random fluctuations close to 0 at longer distances (e.g. alleles *Ha6*^{164}, *Ha6*^{226}, *Ha8*^{156}, *Ha11*^{211}, *Ha11*^{223} and *Ha13*^{178}). Corroborating such general observations of spatial clustering, 23 (46%) significantly positive near-neighbour autocorrelation coefficients (Gabriel-connected graph) were observed (Tables 1 and 2). Note that some high and positive correlations observed at large distances had to be interpreted with caution, mainly because highest distance classes involved a limited number of connected sites to calculate Moran's *I*.

Visual inspection of average *I*-consensus correlograms gave clearer pictures of the underlying spatial structure of allele frequencies (Fig. 3). Such correlograms were suggestive of three different patterns: (i) random fluctuations of Moran's *I* and no evidence of spatial arrangement, e.g. locus *Mdh-1*; (ii) a quasi-continuous decline of autocorrelation, e.g. loci *Ha2*, *Ha8*, *Ha13* and *Lap-2*; (iii) for the other loci, a progressive decrease of average Moran's *I* up to 300–400 m only. The average length of a genetically homogeneous surface (patch size) can be approximated by the *x*-intercept of correlograms (Sokal & Wartenberg 1983; Epperson 1995), and generally ranged from 150 to 250 m. Formal tests for comparing various correlograms were not possible because the statistics for different distance classes are not independent and their effects are unknown (Oden 1984; Epperson 1995).

Barbujani (1987) established a simple relation among the kinship coefficient, Wright's F_{ST} and the Moran's *I* statistics, which allows the estimation of expected values of autocorrelation coefficients under a neutral model of isolation by distance. Using this approach by assuming an exponential decline of genetic similarity in space (according to the Malécot–Morton function), we corroborated the overall fit of allele frequencies to an isolation by distance for all markers, excepted for the locus *Mdh-1* (results not presented).

Spatial differentiation

Whatever the pooling strategy used, hierarchical *F*-statistics indicated in both cases an increase of F_{IS} with population subdivision sizes (Figs 4 and 5). Confidence intervals of the mean values between adjacent levels of grouping always overlapped, and there was no major discontinuity in the increase of F_{IS} values. The relative magnitude of F_{ST} values continuously decreased with pooling stages, a slight increase being nevertheless observed for the last grouping in Fig. 5. Altogether, such results are suggestive of a consistent genetic isolation by distance across the whole area. Similar trends of spatial genetic differentiation were depicted when comparing allozyme and microsatellite loci separately, and no major differences in the interlocus variance have been observed, except for locus *Mdh-1* for which significant genetic differentiation took place only at the first pooling stages. The presence of the road did not affect the results for sequential grouping analyses as well as for spatial autocorrelation analyses (results not shown).

Discussion

Allozyme and microsatellite spatial structure

Assuming that allelic variation is generated under a selectively neutral regime, and that mutation rate is much lower than migration rate, then gene flow and genetic drift are expected to affect all loci uniformly (Sokal & Wartenberg 1983; Sokal *et al*. 1989, 1997; Allendorf & Seeb 2000; Hedrick 2000). The question is whether such conditions are likely to occur in our case study. The answer is largely dependent on the interplay of the time frame in which mutation can act, and the dispersal ability of *Helix aspersa*.

The strong polymorphism displayed by microsatellite loci is primarily due to their high mutation rate (Estoup & Cornuet 1999; Zhu *et al*. 2000). Thus, the different mutation rates of allozymes and tandem repeat of short stretches of DNA could affect the amount of genetic variation between populations, such an effect itself depending on whether differentiation is the result of divergence under complete isolation or mutation-drift equilibrium (Allendorf & Seeb 2000). In addition, discrepancies in number of alleles and heterozygosity can be a source of bias in estimating levels of spatial genetic differentiation among subpopulations (Nagylaki 1998; Hedrick 1999). This concern may be especially crucial when comparing both markers in our study, because of the much greater allelic diversity found at microsatellite loci. However, the two categories of loci displayed similar overall magnitude of genetic differentiation across the sampling site (Arnaud 2000), and followed congruent levels of genetic substructuring according to an isolation by distance model whatever the sequential pooling strategy used. Therefore, spatial autocorrelation analysis showed no major discordance (except for *Mdh-1*, see below) between relative spatial features of genetic distribution across loci. Because of the low divergence time of sampled colonies, migration rate was presumably much larger than mutation rate. As a consequence, the amount of differentiation and

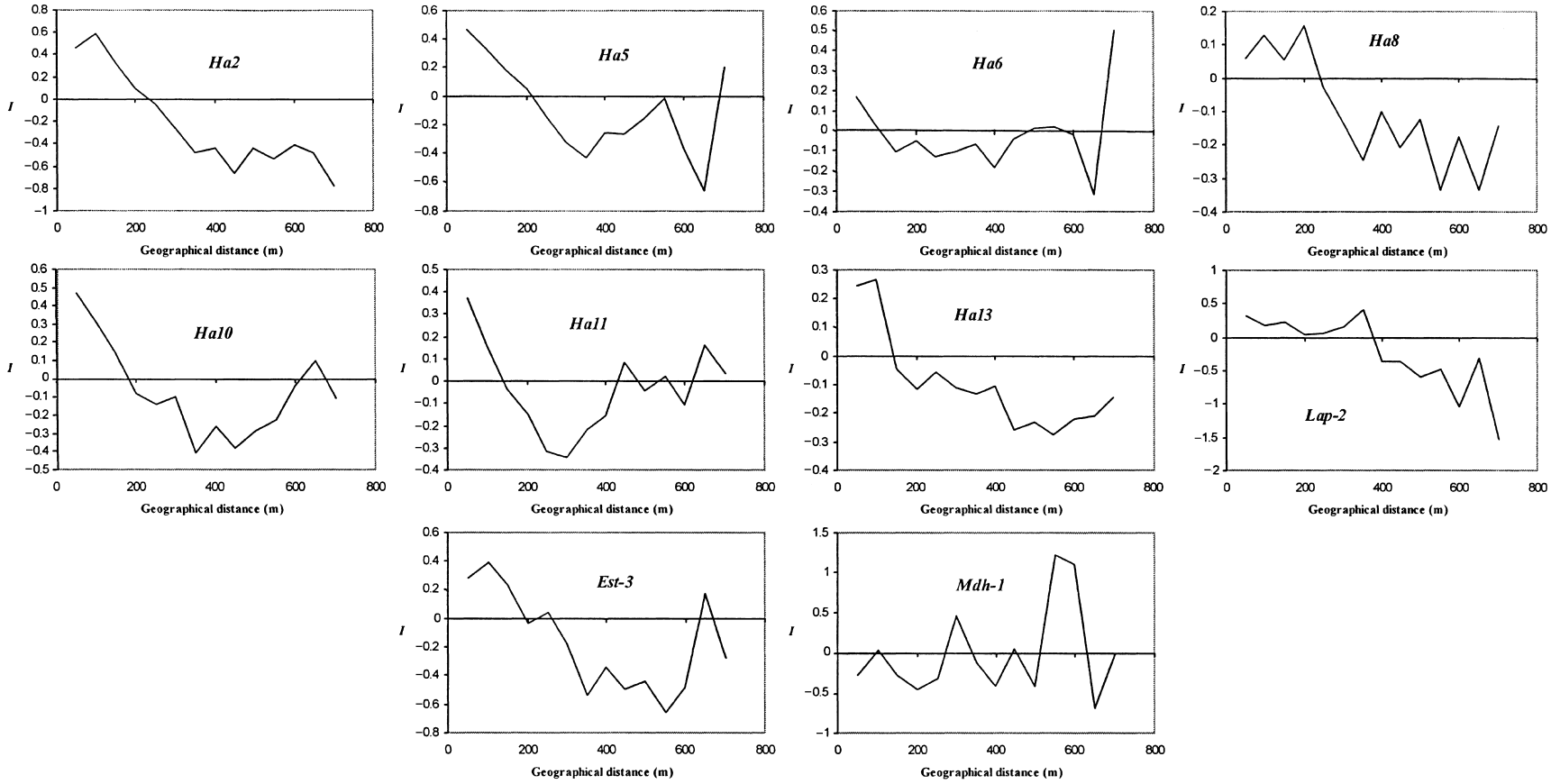

Fig. 3 Microgeographical patterns of genetic variation, as described by consensus correlograms of Moran's *I* values averaged over alleles at each locus in *Helix aspersa*. Significance tests of single-allele estimates used to calculate averages are in Tables 1 and 2. Note that there is no consensus correlograms for *Aat-1* and *Pgm-2* because these loci display only two alleles.

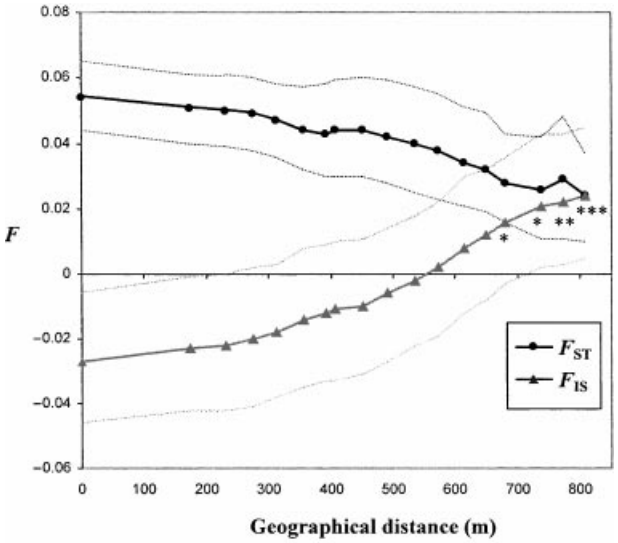

Fig. 4 Variation of F_{ST} and F_{IS} calculated over all loci for successive spatial subdivisions (distance classes in metres) corresponding to sequential pooling of demes in *Helix aspersa* (see text for explanations). Thin lines show the 95% envelope of F_{ST} and F_{IS} obtained by bootstrapping over loci. At each level, F_{ST} values were highly significant; *$P < 0.05$; **$P < 0.01$; ***$P < 0.001$ for F_{IS} values.

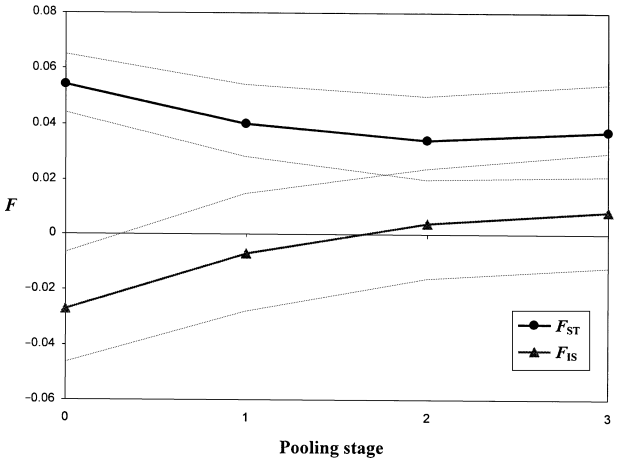

Fig. 5 Changes in F_{ST} and F_{IS} values calculated over all loci when sequentially pooling demes in *Helix aspersa*. Pooling stages are described in the text. Thin lines show the 95% envelope of F_{ST} and F_{IS} obtained by bootstrapping over loci. At each level of variation, all F_{ST} were highly significant ($P < 0.001$) by contrast to F_{IS} values which were not significantly different from 0 for any pooling stage.

its variation over spatial sequential subdivision is best interpreted as a balance between drift and migration, and is apparently not affected by differences in mutation rates between the two classes of markers. With respect to this point, Slatkin & Arter (1991) pointed out that parametric variation, that is the variation in mutation rate between markers, would blur spatial patterns and strongly limit the interest of spatial autocorrelation methods to infer microevolutionary processes. The fact that both kinds of markers overall reveal the same pattern of spatial structure is of interest, because it means that the criticism of Slatkin & Arter (1991) does not apply in our study (see also Hardy & Vekemans 1999).

The scale at which spatial autocorrelation signatures develop depends also on the variability of genetic markers. Despite low numbers of alleles, allozyme markers exhibited relatively high levels of gene diversity. As the spatial genetic arrangement of allozyme frequencies is broadly similar to that observed at microsatellite loci, the strength of spatial signal increases with the level of polymorphism rather than the number of alleles *per se* (see Smouse & Peakall 1999). Can microsatellites nevertheless be considered as much more sensitive indicators of short spatial genetic structuring because of their tendency to have many more alleles? In fact, it has been shown that when allele frequencies decrease below about 0.2–0.1, the degree of autocorrelation and scale of patches both decrease even in a diallelic case (Epperson 1995; Epperson *et al*. 1999). Hence, part of the differences among the two categories of markers may be related to the occurrence of many alleles at low frequencies for microsatellite loci. Such alleles generally tend to be clumped into few colonies. This leads to the shortest *x*-intercepts for single-allele correlograms as well as for some consensus correlograms (e.g. loci *Ha6*, *Ha11*, *Ha13* by contrast to *Lap-2*). Consequently, using microsatellites, there is a higher resolving power in detecting small genetic clustering, mainly because microsatellites drift substantial localized frequencies among colonies.

The salient feature of this spatial analysis is that overall spatial genetic arrangement substantially matched the theoretical predictions based on isolation by distance and the relative dispersal ability of the species. Microevolutionary processes may operate uniformly across loci and should give rise to similar correlogram trends (Sokal & Wartenberg 1983; Sokal *et al*. 1997; Streiff *et al*. 1998). However, contrary to theoretical predictions, spatial structure can be rarely consistent across loci or sites (Smouse & Peakall 1999). Under a dominant genetic isolation by distance process, one would expect that autocorrelation coefficients should decrease monotonically with increasing geographical distance for all loci, which is clearly not the case for *Mdh-1*. This locus exhibited statistically significant heterogeneity in allelic frequencies but lacked spatial arrangement. One possible explanation would simply be related to chance fluctuations in gene frequencies (genetic drift) in each locality that would be quite independent in magnitude and direction from those of neighbouring localities. Indeed, correlograms may be very complex both because of sampling errors and stochastic processes among demes (Slatkin & Arter 1991; Bacilieri *et al*. 1994). Alternatively, selective pressures can also generate distinctive changes in spatial

genetic structure and may be detected through comparisons of spatial autocorrelation statistics for multiple loci (Sokal *et al*. 1989, 1997; Streiff *et al*. 1998; Reusch *et al*. 1999; Ueno *et al*. 2000). However, interferences of selection for adaptive traits due to microsite ecological variations (e.g. Li *et al*. 2000) seem unlikely in our study, because there were no consistent microhabitat heterogeneities except those imposed by the regular spacing of pipes.

Population structure in Helix aspersa

Wright's island model of population genetic structure assumes that parameters such as population size and migration rate are uniform and constant over space and time, under an equilibrium between the homogenizing force of gene flow and diversifying effect of genetic drift. These assumptions are often unrealistic in real populations that are not yet at a genetic equilibrium under their current demographic conditions (Slatkin 1993, 1994; McCauley 1995; Whitlock & McCauley 1999). More realistic, because they incorporate spatial information on interpopulation connectivity, are the stepping-stone model and the isolation by distance model, which predict that the amount of gene flow is expected to decline monotonically with increasing geographical distance between spatially discrete and continuous populations, respectively (Kimura & Weiss 1964; Slatkin 1994; Hamrick & Nason 1996; Sokal *et al*. 1997). Such a situation is likely to occur in *H. aspersa*, the dispersal of which is constrained by distance and where gene flow is most achieved between neighbouring colonies. In agreement with this, patterns identified by spatial autocorrelation analysis were mostly consistent with a gradual microgeographical change in genetic composition, hence reflecting the effects of a limited range of dispersal. Therefore, estimated *F*-values within and among sample demes were strongly influenced by the size of the grouping during the sequential pooling stages. The slight but consistent decrease (increase) of F_{ST} (F_{IS}) values found for most successive pooling levels corroborates that genetic isolation by distance occurs. One can argue that observed *F*-values are difficult to interpret because they correspond to a mixture of different factors affecting the genotypic structure of the population. However, no assumption was made about how and where levels of structuring should be, other than pooling together close geographical sample colonies or according to their genetic affinities. Therefore, because we presumably sampled colonies within the area of one genetic neighbourhood, we avoided the downward bias of population differentiation when the actual populations being compared are themselves composed of genetically distinct entities (i.e. Wahlund effect). Hence, the estimated *F*-statistics over different groupings are a combination of both the within-population genetic composition due to the breeding behaviour of *H. aspersa*, and the among-subpopulation heterozygote deficit due to the Wahlund effect (Bacilieri *et al*. 1994; Goudet *et al*. 1994). The magnitude of the F_{IS} increase is quite low and suggests that gene flow acts as an effective homogenizing factor, at least for more closely situated colonies.

In contrast to the *F*-statistics, spatial autocorrelation methods account for information from all pairs of localities, make no assumption regarding the underlying population genetic model, and have been successful even in populations where structure is very weak (Bacilieri *et al*. 1994; Epperson *et al*. 1999; Reusch *et al*. 1999). Here, positive autocorrelation of short distance classes probably reflects genetic clustering and family structures caused by limited short-range dispersal. Marked homing behaviour may also contribute to the development of genetically distinct patches of individuals (e.g. Selander & Kaufman 1975).

An isolation by distance model produces intermediate levels of long-distance gene flow compared with both stepping-stone and island models of population structure (Hamrick & Nason 1996). A continuous decreasing set of autocorrelation coefficients across all distance classes describes a genetic gradient (Chikhi *et al*. 1998; Casalotti *et al*. 1999), as shown by locus *Ha2* (see Table 1). By contrast, interaction of short-range gene flow and genetic drift under an isolation by distance is reflected in an asymptotic decline of autocorrelation from positive significant to insignificant coefficients at far distances (Barbujani 1987; Chikhi *et al*. 1998; Casalotti *et al*. 1999), which is clearly the case for loci *Ha10* or *Ha11* (see Fig. 3). More precisely, the inspection of consensus correlograms allows us to discriminate the precise features of such microevolutionary processes: spatial signatures of *Ha5*, *Ha6*, *Ha10*, *Ha11*, or *Est-3* consensus correlograms can be viewed as the expression of a generalized stepping-stone model, whereas those obtained for loci *Ha2*, *Ha13*, or *Lap-2* are more consistent with a stepping-stone including an external migrational scenario (see Sokal *et al*. 1997; p. 87).

However, attempts to interpret population differentiation in terms of evolutionary and ecological causes may lead to erroneous conclusions in the absence of historical considerations. The area under study is subject to recurrent human disturbances (herbicide and pesticide treatments) responsible for some fluctuations in effective population size, population crashes, or localized extinctions (Arnaud 2000). Such effects, leading to an altered isolation by distance where more distantly separated colonies are predominantly influenced by genetic drift, can be visualized by a greater stochasticity in the Moran's *I* fluctuations for the longest distance classes (e.g. locus *Ha8*). Another point is the time needed for a spatial genetic structure to reach an equilibrium state between the loss of alleles due to drift and their replacement by migration, so that in a newly settled area, the detection of a well-established isolation by distance model can be quite difficult (Slatkin 1993; Hutchison & Templeton 1999; Whitlock & McCauley 1999).

Altogether, our results are consistent with a neighbourhood structure of randomly mating hermaphrodites where more closely situated colonies tend to be more genetically similar to one another. Some degree of association between genetic distribution and geographical distance is related to the increased likelihood of dispersal between adjacent colonies, following a step-by-step relationship pattern (Arnaud *et al*. 1999b). As shown in other Gastropod species, such as *Albinaria corrugata* (Schilthuizen & Lombaerts 1994), gene flow acts as an effective factor for shortest scale of investigation. Beyond this level, local colonies can be considered as relatively independent units and genetic drift drives the spatial genetic differentiation among these colonies. Finally, microsatellite loci are especially suitable markers for the detection of minor changes in genetic composition, as expected under the neighbourhood model (Pfenninger *et al*. 1996), and hold the potential for analysis of the evolutionary history of populations over short temporal and geographical scales.

Acknowledgements

We are grateful to L. Excoffier and two anonymous reviewers for insightful and critical comments that greatly improved this manuscript.

References

Allendorf FW, Seeb LW (2000) Concordance of genetic divergence among sockeye salmon populations at allozyme, nuclear DNA, and mitochondrial DNA markers. *Evolution*, **54**, 640–651.

Arnaud J-F (2000) *Organisation spatiale de la variabilité génétique dans une métapopulation de l'escargot terrestre* Helix aspersa *(Gastropoda: Pulmonata)*. PhD Thesis. Université de Rennes (Rennes 1), France.

Arnaud J-F, Madec L, Daguzan J (1999a) Spatial differentiation of allozyme frequencies in a subdivided population of the land snail *Helix aspersa*. *Journal of Molluscan Studies*, **65**, 267–271.

Arnaud J-F, Madec L, Bellido A, Guiller A (1999b) Microspatial genetic structure in the land snail *Helix aspersa* (Gastropoda: Helicidae). *Heredity*, **83**, 110–119.

Bacilieri R, Labbe T, Kremer A (1994) Intraspecific genetic structure in a mixed population of *Quercus petraea* (Matt.) Leibl and *Q. robur* L. *Heredity*, **73**, 130–141.

Barbujani G (1987) Autocorrelation of gene frequencies under isolation by distance. *Genetics*, **117**, 777–782.

Casalotti R, Simoni L, Belledi M, Barbujani G (1999) Y-chromosome polymorphisms and the origins of the European gene pool. *Proceedings of the Royal Society of London B*, **266**, 1959–1965.

Chapuisat M, Goudet J, Keller L (1997) Microsatellites reveal high population viscosity and limited dispersal in the ant *Formica paralugubris*. *Evolution*, **51**, 475–482.

Chikhi L, Destro-Bisol G, Bertorelle G, Pascali V, Barbujani G (1998) Clines of nuclear DNA markers suggest a largely Neolithic ancestry of the European gene pool. *Proceedings of the National Academy of Sciences of the USA*, **95**, 9053–9058.

Denny M (1980) Locomotion: the cost of gastropod crawling. *Science*, **208**, 1288–1290.

Epperson BK (1995) Spatial distributions of genotypes under isolation by distance. *Genetics*, **140**, 1431–1440.

Epperson BK, Huang Z, Li TQ (1999) Measures of spatial structure in samples of genotypes for multiallelic loci. *Genetical Research*, **73**, 251–261.

Estoup A, Cornuet J-M (1999) Microsatellite evolution: inferences from population data. In: *Microsatellites: Evolution and Applications* (eds Goldstein DB, Schlötterer C), pp. 49–65. Oxford University Press, Oxford.

Estoup A, Largiader CR, Perrot E, Chourrout D (1996) Rapid one-tube DNA extraction for reliable PCR detection of fish polymorphic markers and transgenes. *Molecular Marine Biology and Biotechnology*, **5**, 295–298.

Gabriel KR, Sokal RR (1969) A new statistical approach to geographic variation analysis. *Systematic Zoology*, **18**, 259–278.

Goudet J (1995) FSTAT (Version 1.2). A computer program to calculate *F*-statistics. *Journal of Heredity*, **86**, 485–486.

Goudet J, De Meeüs T, Day AJ, Gliddon CJ (1994) The different levels of population structuring of the dogwhelk, *Nucella lapillus*, along the South Devon coast. In: *Genetics and Evolution of Aquatic Organisms* (ed. Beaumont AR), pp. 81–95. Chapman & Hall, London.

Guiller A, Madec L, Daguzan J (1994) Geographical patterns of genetic differentiation in the landsnail *Helix aspersa* Müller (Gastropoda: Pulmonata). *Journal of Molluscan Studies*, **60**, 205–221.

Guiller A, Arnaud J-F, Vautrin D, Solignac M (2000) Highly polymorphic microsatellite markers in the land snail *Helix aspersa* (Gastropoda: Pulmonata). *Molecular Ecology*, **9**, 1191–1193.

Hamrick JL, Nason JD (1996) Consequences of dispersal in plants. In: *Population Dynamics in Ecological Space and Time* (eds Rhodes OE, Chesser RK, Smith MH), pp. 203–236. University of Chicago Press, Chicago.

Hardy OJ, Vekemans X (1999) Isolation by distance in a continuous population: reconciliation between spatial autocorrelation analysis and population genetics models. *Heredity*, **83**, 145–154.

Hedrick PW (1999) Highly variable loci and their interpretation in evolution and conservation. *Evolution*, **53**, 313–318.

Hedrick PW (2000) *Genetics of Populations*. 2nd edn. Jones and Bartlett Publishers Inc., Sudbury, MA.

Hutchison DW, Templeton AR (1999) Correlation of pairwise genetic and geographic distance measures: inferring the relative influences of gene flow and drift on the distribution of genetic variability. *Evolution*, **53**, 1898–1914.

Kimura M, Weiss GH (1964) The stepping-stone model of population structure and the decrease of genetic correlation with distance. *Genetics*, **49**, 561–576.

Kirchman JJ, Whittingham LA, Sheldon FH (2000) Relationships among cave swallow populations (*Petrochelidon fulva*) determined by comparisons of microsatellite and cytochrome b data. *Molecular Phylogenetics and Evolution*, **14**, 107–121.

Lamotte M (1951) Recherches sur la structure génétique des populations naturelles de *Cepaea nemoralis* (L.). *Bulletin Biologique de la France et de la Belgique*, **35** (Suppl.), 1–239.

Li YC, Fahima T, Korol AB, *et al*. (2000) Microsatellite diversity correlated with ecological-edaphic and genetic factors in three microsites of wild emmer wheat in north Israel. *Molecular Biology and Evolution*, **17**, 851–862.

Madec L (1991) Genetic divergence in natural populations of the land snail *Helix aspersa* Müller, 1774. *Journal of Molluscan Studies*, **57**, 483–487.

Madec L, Desbuquois C, Coutellec-Vreto M-A (2000) Phenotypic plasticity in reproductive traits: importance in the life history of

Helix aspersa (Mollusca: Helicidae) in a recently colonized habitat. *Biological Journal of the Linnean Society*, **69**, 25–39.

McCauley DE (1995) Effects of population dynamics on genetics in mosaic landscapes. In: *Mosaic Landscapes and Ecological Processes* (eds Hansson L, Fahrig L, Merriam G), pp. 178–198. Chapman & Hall, London.

Nagylaki T (1998) Fixation indices in subdivided populations. *Genetics*, **148**, 1325–1332.

Oden NL (1984) Assessing the significance of a spatial correlogram. *Geographical Analysis*, **16**, 1–16.

Pfenninger M, Bahl A, Streit B (1996) Isolation by distance in a population of small land snail *Trochoidea geyeri*: evidence from direct and indirect methods. *Proceedings of the Royal Society of London B*, **263**, 1211–1217.

Reusch TBH, Hukriede W, Stam WT, Olsen JL (1999) Differentiating between clonal growth and limited gene flow using autocorrelation of microsatellites. *Heredity*, **83**, 120–126.

Rudman B (1999) Introduced snails in Australia. *Australian Museum Web Site*.

Schilthuizen M, Lombaerts M (1994) Population structure and levels of gene flow in the mediterranean land snail *Albinaria corrugata* (Pulmonata: Clausiliidae). *Evolution*, **48**, 577–586.

Selander RK, Kaufman DW (1975) Genetic structure of populations of the brown snail (*Helix aspersa*). I. Microgeographic variation. *Evolution*, **29**, 385–401.

Selander RK, Ochman H (1983) The genetic structure of populations as illustrated by Molluscs. In: *Isozymes: Current Topics in Biological and Medical Research, Vol. 10, Genetics and Evolution* (eds Rattazzi MC, Scandalios JG, Whitt GS), pp. 93–123. Alan R. Liss, Inc., New York.

Slatkin M (1993) Isolation by distance in equilibrium and non-equilibrium populations. *Evolution*, **47**, 264–279.

Slatkin M (1994) Gene flow and population structure. In: *Ecological Genetics* (ed. Real LA), pp. 3–17. Princeton University Press, Princeton, NJ.

Slatkin M, Arter HE (1991) Spatial autocorrelation methods in population genetics. *American Naturalist*, **138**, 499–517.

Smouse PE, Peakall R (1999) Spatial autocorrelation analysis of individual multiallele and multilocus genetic structure. *Heredity*, **82**, 561–573.

Sokal RR, Oden NL (1978) Spatial autocorrelation in biology 1. Methodology. *Biological Journal of the Linnean Society*, **10**, 199–228.

Sokal RR, Wartenberg DE (1983) A test of spatial autocorrelation analysis using an isolation-by-distance model. *Genetics*, **105**, 219–237.

Sokal RR, Jacquez GM, Wooten MC (1989) Spatial autocorrelation analysis of migration and selection. *Genetics*, **121**, 845–855.

Sokal RR, Oden NL, Thomson BA (1997) A simulation study of microevolutionary inferences by spatial autocorrelation analysis. *Biological Journal of the Linnean Society*, **60**, 73–93.

Streiff R, Labbe T, Bacilieri R, Steinkellner H, Glössl J, Kremer A (1998) Within-population genetic structure in *Quercus robur* L. & *Quercus petraea* (Matt.) Liebl. assessed with isozymes and microsatellites. *Molecular Ecology*, **7**, 317–328.

Takahashi M, Mukouda M, Koono K (2000) Differences in genetic structure between two Japanese beech (*Fagus crenata* Blume) stands. *Heredity*, **84**, 103–115.

Ueno S, Tomaru N, Yoshimaru H, Manabe T, Yamamoto S (2000) Genetic structure of *Camellia japonica* L. in an old-growth evergreen forest, Tsushima, Japan. *Molecular Ecology*, **9**, 647–656.

Weir BS, Cockerham CC (1984) Estimating *F*-statistics for the analysis of population structure. *Evolution*, **38**, 1358–1370.

Whitlock MC, McCauley DE (1999) Indirect measures of gene flow and migration: $F_{ST} \neq 1/(4Nm + 1)$. *Heredity*, **82**, 117–125.

Williams CF, Waser NM (1999) Spatial genetic structure of *Delphinium nuttallianum* populations: inferences about gene flow. *Heredity*, **83**, 541–550.

Zhu Y, Queller DC, Strassmann JE (2000) A phylogenetic perspective on sequence evolution in microsatellite loci. *Journal of Molecular Evolution*, **50**, 324–338.

This work was part of Jean-François Arnaud's doctoral research under the supervision of Luc Madec and Annie Guiller. J.-F.A.'s PhD project focuses on population genetics in the garden snail *Helix aspersa*, within a recently invaded agricultural area where this snail fits a metapopulation structure with recurrent population turnovers mediated by human activity. L.M. works on the evolution of phenotypic plasticity in reproductive traits and its consequences in the life history of *H. aspersa*. His other research interest is the study of shell variation in land snails. A.G. is undertaking a vast phylogeographical reconstruction of the evolutionary history of *H. aspersa* in Maghreb and Western Europe using molecular markers. A.B. currently develops statistical methods for multivariate analysis and improves its software package for spatial analysis of genetic diversity.
